

Elucidation of Biological Activity of Silver Based Nanoparticles Using Plant Constituents of *Syzygium cumini*

Disha Mittal¹, Kritika Narang^{1,2}, Ankita Leekha¹, Kapinder Kumar¹ and Anita Kamra Verma^{1,*}

¹Nanobiotech lab, Department of Zoology, Kirori Mal College, University of Delhi, P.O.Box 110007, Delhi, India.

²Department of Physics and Astrophysics, University of Delhi, P.O.Box 110007, Delhi, India.

(*) Corresponding author: akamra23@hotmail.com

(Received: 03 September 2018 and Accepted: 04 December 2018)

Abstract

We report the efficacy of the silver nanoparticles (AgNPs) synthesized using the leaf and bark extracts of *Syzygium cumini* (common name Jamun) with silver nitrate (AgNO_3) which were used as both reducing and capping agent at varied temperatures- 25°C, 37°C and 80°C. Three sets of AgNPs from leaf and bark extracts, were synthesized at the above mentioned temperatures, and then physical characterization using UV-Vis spectroscopy indicated a peak in the range of 385-460nm. The hydrodynamic radii measured by DLS clearly indicated the size of AgNPs in the range of 72-284nm. The biological efficacy in terms of antimicrobial activity was assessed by Kirby Bauer method, applied for both Gram positive and Gram negative bacteria such as *Staphylococcus aureus* and *Escherichia coli* respectively. The Zone of inhibition (ZOI) diameter was found to be 22mm and 20mm in *S.aureus* and *E.coli*, indicated the bactericidal activity of AgNPs synthesized from leaf extract at 25°C was maximum. Further, the IC_{50} of the same AgNP was 12.5µg/ml indicating 49.3% cytotoxicity in human breast adenocarcinoma cell line MCF-7 confirmed the anticancer activity, whereas in HEK cell line the cytotoxicity observed was only 8.95% at the same concentration. The upregulation of apoptotic marker "p53" post treatment with 12.5µg/ml for 24hrs as done by Western blotting. Hence, AgNPs synthesized by green synthesis are proposed as economical, environment friendly having immense potential for drug delivery.

Keywords: Anticancer, Antimicrobial, Apoptosis, Green chemistry, Silver Nanoparticles, *Syzygium cumini*.

1. INTRODUCTION

Nanoparticles tend to acquire unique characteristics owing to their increased surface area to volume ratio translating into enhanced anti-microbial and optical properties, coupled with structural strength enhancement properties [1]. Nanoparticles may be broadly divided into an organic group that includes carbon nanoparticles (fullerenes), and inorganic group that comprises of noble metal nanoparticles (silver and gold), magnetic nanoparticles and semi-conductor nanoparticles - zinc oxide and titanium oxide. Inorganic nanoparticles of noble metals are gaining popularity as they provide superior physical properties coupled with functional

versatility [2]. Among the metal nanoparticles, silver nanoparticles (AgNPs) have generated sufficient interest due to its chemical stability, enhanced conductivity, catalytic and most important antibacterial, anti-fungal, anti-viral, anti-cancer anti-inflammatory activities which can be integrated into composite fibres, cosmetic products, cryogenic superconductors, food industry and electronic components[3-4]. AgNPs have been used for defense against a variety of micro-organisms, and further to combat drug resistance in microbes. AgNPs have remarkable properties that can be exploited for wastewater treatment,

agriculture, drug delivery and biomedical applications.

Metal nanoparticles can be synthesized by both chemical and physical methods including electrochemical reduction [5], chemical reduction [6], heat evaporation [7] and photochemical reduction [8]. Other protocols like gamma radiation, laser ablation, micro emulsion, autoclave and microwaving are efficient methods too, but are limited by high operational costs, energy consumption and use of toxic chemicals [9]. In such a scenario, green synthesis has tremendous potential as it is cost effective, environment friendly coupled with an ease of scaling up [3]. Green synthesis would greatly rely on selection of the plant to be used as the reducing agents like citric acid, flavonoids, ascorbic acids, dehydrogenases, reductases and extracellular electron shuttlers that play an essential role for biosynthesis of metal nanoparticles [2]. Plant extracts acts as a reducing and capping agent forming stable and shape controlled AgNPs [10]. The plant borne biomolecules include reducing agents like enzymes, amino acids, proteins, polysaccharides, vitamins, and organic acids such as citrates that are environmentally benign, yet chemically complex [11].

In the present work we propose to synthesize AgNPs from *S. cumini* leaves and bark by the use of chemicals, as the leaves itself contain betulinic acid, β -sitosterol, mycaminose, crategolic (maslinic) acid, n-hepatcosane, n-hentriacontane, n-nonacosane, n-dotricontanol, n-octacosanol, n-triacontanol, myricitrin, quercetin, myricetin and the flavonol glycosides myricetin 3-O-(4"-acetyl)- α L-rhamnopyranosides. The stem contains betulinic acid, friedelan-3- α -ol, Friedelin, gallic acid, kaempferol, β -sitosterol, ellagic acid, β -sitosterol-D glucoside, ellagitannin and gallotannin, and myricetin [12] that may act as a reducing agent during the synthesis of AgNPs.

Temperature dependent synthesis and characterization of AgNPs from extracts of

leaf and bark of *S. cumini* in terms of its biological efficacy against *S. aureus* and *E. coli* were evaluated. We further report its biotoxicity at the cellular level in normal HEK and MCF-7 breast cancer cell lines.

2. EXPERIMENTAL

2.1 Materials

Fresh leaves and bark were obtained from the *S. cumini* tree located in the Institution itself. Nutrient agar, Nutrient broth, Gentamycin, Fetal Bovine Serum (FBS), Dulbecco's Modified Eagles's Medium (DMEM), Antibiotic-Antimycotic solution (Streptomycin/Pencillin), Phosphate Buffer saline (PBS), skimmed milk, Hydroxyl ethyl piperazine ethane sulphonic acid (HEPES), Luria-Bertani Broth were purchased from Hi-Media Laboratories Pvt Ltd(Mumbai,India). Silver nitrate (AgNO_3) Ethidium bromide(EtBr), Dimethyl sulph-oxide (DMSO), Sodium bicarbonate, NP-40, Agarose, TritonX-100, Tween-20, 3-(4,5-Dimethyl-thiazol -2-yl)-2,5-Diphenyl tetrazolium Bromide [MTT] were all purchased from Sigma-Aldrich (USA). Primary antibodies anti-mouse: β -actin [(C4): sc-47778], p53 [(DO-1): sc-126] and secondary antibody: goat anti-mouse Ig-HRP (sc-2005) were procured from Santa Cruz Biotechnology. Chloroform, Isoamyl alcohol, Phenol, Sodium Chloride, Ethylene diamine tetraacetic acid (EDTA), Tris-HCl were obtained from SRL, India. All the chemicals were used without further purification.

2.2 Synthesis of AgNPs

Leaves and bark were scrupulously washed with distilled water and left for air drying. Briefly, 3g of dried leaves and bark were weighed separately and dissolved in 30 ml of distilled water and kept at 80°C for 1hr. The extracts thus prepared were cooled and filtered through Whatmann's Filter paper no. 1 and stored at 4°C. To 45ml of 1mM AgNO_3 , 5 ml of the above prepared leaf and bark extract were added drop wise under vigorous stirring and

maintained at three different temperatures: 25°C, 37°C and 80°C. Change in colour was observed slowly from transparent to brown, that indicated the formation of AgNPs.

2.3 Characterization of AgNPs

2.3.1 UV Visible Spectral Analysis

Although, color change is an indicator of nanoparticle formation, it cannot be the sole, reliable parameter indicating formation of AgNPs, hence the shift in the absorption spectra for AgNPs as observed by UV-Spectrophotometer (Cary-60, Agilent Technologies, USA). The shift in the absorbance spectra indicated the formation of nanoparticles and was compared to spectra of distilled water taken as blank.

2.3.2 Dynamic Light Scattering

The hydrodynamic radii were analyzed by Dynamic light Scattering (DLS) using Zeta-sizer (Nano-ZS, Malvern USA). For the size based assessment of nanoparticles the sample solution was diluted (1:9) with deionized water.

2.3.3 Transmission Electron Microscopy

Transmission Electron Microscopy (TEM) was done to examine the size and morphology of the AgNPs. A drop of aqueous solution containing the AgNPs, was placed on the carbon coated copper grid and dried under Infra-red lamp. The carbon coated grids were observed under Technai G² T-30U-TWIN of FEI.

2.3.4 FTIR Analysis

FTIR was used to identify and analyze the functional group and composition of the lyophilized AgNPs responsible for the reduction of Ag ion and capping of the bio-reduced silver nanoparticles. using Cary 630 FTIR (Agilent Technologies). The sample was placed on the diamond ATR of the instrument and the peaks were observed using the MicrolabPC software.

2.3.5 Disc Diffusion Assay

As per previously published protocol of Dey *et al* 2015 [13], nutrient broth was prepared and autoclaved at a temperature of 121°C and pressure of 15 lb/in², for 20 min. Mother inoculum for both bacterial cultures (*S.aureus* ATCC no. 25923 and *E.coli* DH5 α ATCC no. 67877) were taken in 1:100 ratios and sterile broth was inoculated. The flasks were then incubated overnight in the orbital shaker at 37°C. After 24 hrs of incubation, the turbidity confirmed the growth of the culture in the media. The absorbance at 600 nm was measured in UV spectrophotometer and CFU/ml was calculated as:

$$1\text{OD (Optical Density)} = 0.8 \times 10^9 \text{ CFU/ml.} \dots\dots\dots (i)$$

The susceptibility of AgNPs against bacteria was assessed by Kirby Bauer method. Briefly, LB agar plates were prepared and the soft agar containing the bacterial suspension was poured on it. Sterile discs of Whatmann filter paper were then kept on each section, laden with 20 μ l of AgNPs [synthesized from *S. cumini* leaves at 25°C, 37°C, 80°C (Group I) and from *S. cumini* bark at 25°C, 37°C and 80°C (Group II)], AgNO₃, Gentamycin (1 mg/ml) was used here as a positive control and distilled water as a negative control. The plates were then sealed with parafilm and were incubated at 37°C overnight. The zone of inhibition (ZOI) was observed post 24 hrs and measured subsequently.

2.3.6 Maintenance of Mammalian cells

The Human breast adenocarcinoma cell-line (MCF-7) and Human embryonic Kidney cell-line (HEK) were cultured in DMEM with 10% Fetal Bovine serum (FBS) supplement with antibiotic solution (100 U/ml penicillin and 100 μ g/ml streptomycin). The cells were grown in a humidified atmosphere of 5% CO₂ at 37°C in a CO₂ incubator (Thermo).

2.3.7 Biototoxicity Assay

The cytotoxicity of AgNPs synthesized from *S. cumini* leaves at 25°C were

examined as per previously published protocol [14]. Percent cytotoxicity studies were evaluated on MCF-7 and HEK cells by the MTT assay. Briefly, 5×10^3 cells/well were seeded in a 96-well microtiter plate, supplemented with 10% FBS. Next day the cells were given a treatment with Leaf extract (L.E.) and AgNPs synthesized from *S. cumini* leaves extract at 25°C at five concentrations i.e. 100 µg/ml, 50 µg/ml, 25 µg/ml, 12.5 µg/ml, 6.25 µg/ml for 24 hrs. After the requisite time period, 20 µl of MTT solution (5 mg/ml in PBS pH 7.4) was added to each well and incubated at 37°C for 4 hrs. The formazan crystals so formed were further dissolved in DMSO. The O.D was measured at 540 nm on an ELISA reader plate (Synergy HT, BioTek, USA) after mixing on a mechanical plate mixer. All the measurements were done in triplicates. The colour so developed was directly proportional to the number of viable cells. IC₅₀ values were determined for all samples at the end of 24 hrs and the percent (%) cytotoxicity was using the calculated using described formula:

$$\% \text{ Cytotoxicity} = \frac{([A]_{\text{control}} - [A]_{\text{test}})}{[A]_{\text{control}}} \times 100 \dots \dots \dots (ii)$$

Where,

[A]_{test} = Absorbance of the sample to be tested

[A]_{control} = Absorbance of the control sample.

2.3.8 Western Blotting

1×10^6 cells were seeded in DMEM media, supplemented with 10% FBS and then incubated with AgNPs synthesized from *S. cumini* leaves at 25°C for 24 hrs. Next day, the cells were harvested and washed in PBS twice and then lysed with lysis buffer for 30 min on ice. The lysate was centrifuged at 15000 rpm for 15 min. The supernatant was taken and protein concentration was measured by CB Assay reagent kit at 595 nm. Briefly, 80µg/ml of protein was loaded in equal amounts on 15% SDS-PAGE gel. The separated proteins were then transferred to a

nitrocellulose membrane followed with a blocking step using 5% BSA (Bovine Serum Albumin) in TBS with tween-20 (TBS-T) for 2 hrs. It was further incubated with p53 (1:1000 dilutions) for another two hours. Thereafter, the membrane was washed thrice with TBST (30 minutes) and incubated 2hrs with 1:500 times diluted secondary antibody (goat anti-mouse conjugated with horseradish peroxidase), subsequently. The bands were analyzed using a freshly prepared developer solution of DAB [15] and normalized to a β-actin control.

3. RESULTS AND DISCUSSION

Various plant parts have been used for the green synthesis of metal nanoparticles. Synthesis of AgNP in colloidal form is most commonly done by reduction of the silver nitrate. The possible mechanism involves the formation of intermediary complexes with the phenolic -OH groups present on the hydrolysable tannins, undergoing an oxidation reaction to quinone followed by reduction of AgNPs from Ag⁺ [16]. Figure 1 indicates the UV absorption spectra of AgNPs. The formation of AgNPs is characterized by a change from colorless AgNO₃ to a brownish solution. The appearance of the brown color was a result of the excitation of surface plasmon resonance (SPR), majorly of AgNPs having the λ_{max} in the range of 385-460 nm (Table 1). Figure 2 represents the UV absorption spectra of both leaf and bark extract. On examining AgNP, it was observed that the intensity of the peak was directly proportional to the reaction time, which may be due to the formation of AgNPs during the reaction. It has already been proved that the intensity of the Surface Plasmon peak was directly related to the density of the NPs in solution [17]. The observed SPR was in the range of 385-460 nm and the broadening of the peak indicated the polydispersity of AgNPs [18]. Formation of stable AgNPs within an hour proves this method to be an efficient bio-reducing method for synthesizing Ag

nanostructures [19-20]. We have also observed the instability of the peak of the nanoparticles at higher temperatures i.e. 80°C. The synthesis was done at three temperatures i.e. 25°C, 37°C, and 80°C. As 25°C is the ambient temperature, 37°C is the physiological temperature and at 80°C the extract had been prepared at this temperature. Therefore,

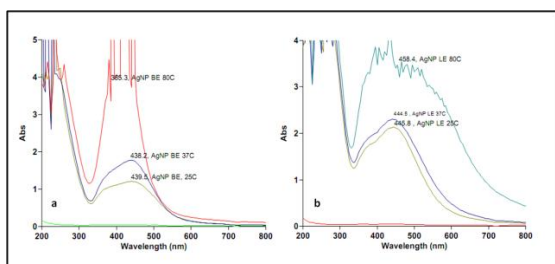


Figure 1. UV-Vis Spectra of AgNP prepared from a) Leaf Extract at 25°C, 37°C, 80°C b) Bark Extract 25°C, 37°C, 80°C

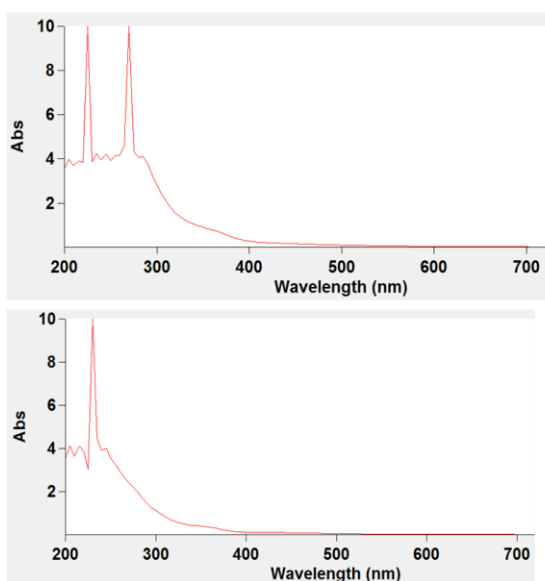


Figure 2. UV-Vis Spectra of a) Leaf Extract b) Bark Extract.

Table 1. UV-VIS absorption peak of AgNPs.

S.No.	Extract used	Temp. of synthesis (°C)	λ_{max} (nm)
1.	Leaf	25	439.5
2.	Leaf	37	438.2
3.	Leaf	80	385.3
4.	Bark	25	445.8
5.	Bark	37	444.5

6.	Bark	80	458.4
----	------	----	-------

Figure 3 represents temperature dependent variation in the size of the nanoparticles by dynamic light scattering (DLS) and transmission electron microscopy (TEM) techniques (Figure 4). Table 2 represents the size of the AgNPs, wherein, it was observed that AgNPs derived from bark extract were smaller in size when compared to that of leaf extract. AgNPs were in the range of ≤ 50 nm having a spherical morphology (Figure 4). Hence, the TEM results were anomalous with the DLS results. The differences most likely indicates the fact that TEM measures a number based size distribution of the physical size only. However, DLS is very sensitive to even small quantity of large particles which maybe a result of nanoparticles aggregating or possibly a contamination and thus the DLS peaks are indicating larger sizes. Large particle size in DLS data could be due to hydrodynamic circumference and interaction in various forces in ionic condition. [21].

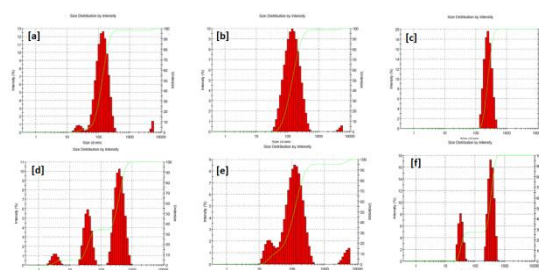


Figure 3. Size of AgNPs prepared from (a) Leaf Extract at 25°C (b) Leaf Extract at 37°C, (c) Leaf Extract at 80°C (d) Bark Extract 25°C, (e) Bark Extract at 37°C, (f) Bark Extract at 80°C.

Table 2. Size of different AgNPs prepared from different extracts.

S.No.	Extract used	Temp. of synthesis (°C)	Average size (nm)	PDI
1.	Leaf	25	125.3	0.325
2.	Leaf	37	122.8	0.261
3.	Leaf	80	273.8	0.280
4.	Bark	25	72.02	0.896
5.	Bark	37	84.92	0.458

6.	Bark	80	284.3	0.533
----	------	----	-------	-------

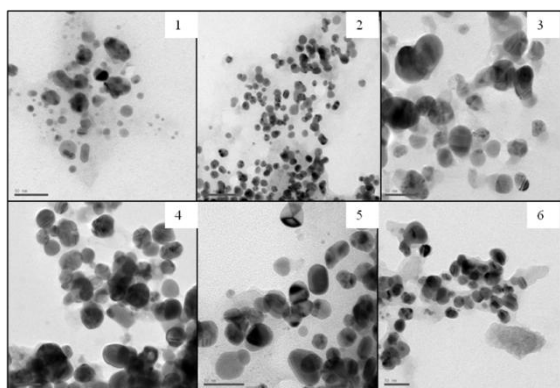


Figure 4. TEM images of AgNPs synthesized from (a)Bark Extract at 1)25°C, 2) 37°C, (3)80°(b)Leaf Extract (4)25°C, (5)37°C, (6) 80°C

Earlier reports also supports our results indicated that particle size distribution in DLS data showed size range 70 nm - 125nm, whereas TEM data showed 20 nm - 50 nm.

Since, the nanoparticles possess a large surface area, the surface modification by a suitable adsorbate can produce different properties, hence FTIR spectroscopy was used for the detection of functional groups in pure compounds, mixtures and for comparison among compounds, that correlated with the vibrational motion of atoms or molecules. Figure 4 a, b, c depicted the AgNP synthesized from *S.cumini* leaf extract has -CHO peak around 2900 cm^{-1} , C-O stretch of alcohol group at 1100 cm^{-1} and have three peaks depicting amines groups i.e C-N stretch at 1030 cm^{-1} , Ar-N stretch at 1320 cm^{-1} and NH_2 in plane bend at 1610 cm^{-1} (Fig 5) where as graph d, e, f depicted the AgNP synthesized from *S. cumini* bark extract which has peaks at $\sim 2100\text{ cm}^{-1}$ representing C \equiv C stretch, at NH_2 in plane bend at 1610 cm^{-1} , 1037 cm^{-1} represented NH_2 group and benzene at $\sim 829\text{ cm}^{-1}$ (Figure 6). As per Siddig et al. 2015, FTIR analysis of *S. cumini* leaf and bark indicated a broad and strong absorption band in a range of $685\text{-}1638\text{ cm}^{-1}$ [22]. These absorptions are allocated to different stretching vibrations. The C-C, O-H

stretching vibration were appeared at 685 cm^{-1} , 1633 cm^{-1} and 3400 cm^{-1} , respectively. Further, the C=O stretching was observed at 1400 cm^{-1} . The FTIR of all the six prepared AgNPs were almost similar. After the formation of AgNP there was a decrease in the region of $1600\text{-}1500\text{ cm}^{-1}$ that indicated the involvement of aromatic compounds in the reduction process, thereby confirming the formation of AgNPs.

Antimicrobial disc diffusion assay of all the six variants of prepared nanoparticles were done (Table 3) (Figure 7) and maximum activity was shown by AgNPs synthesized from leaf extract at 25°C against both the type of bacteria whether Gram positive (*S.aureus*) or Gram negative (*E.coli*) bacteria. The bactericidal effect of the AgNPs at 100 ng/ml was observed in *S.aureus*, but at the same dose of AgNPs in *E.coli* exhibited a bacteriostatic effect (Table 4).

It had been earlier reported that AgNPs were capable of adhering to the bacterial cell wall and penetrating it, causing conformational changes in the cell membrane ultimately leading to cell death [23]. Published evidences indicated strong interaction between AgNPs and the peptidoglycan (PGN).

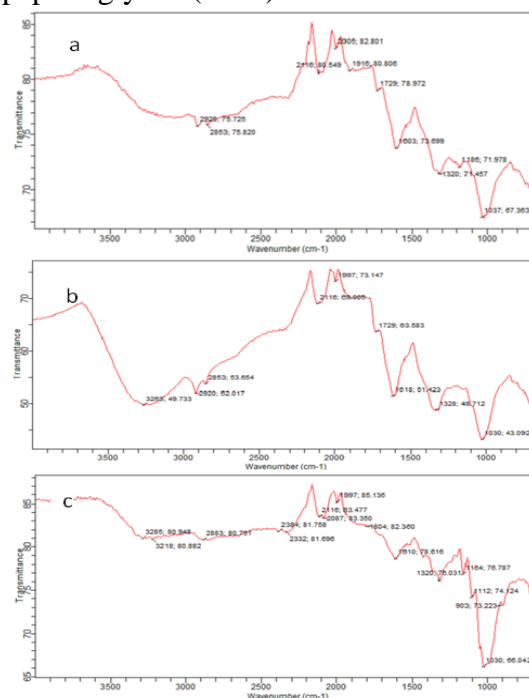


Figure 5. FTIR of AgNPs synthesized from Leaf Extract (a)25°C, (b)37°C, (c) 80°C

Table 3. Zone of inhibition (diameter in mm) of different samples

Sample no. in plate	Sample	ZOI in <i>S.aureus</i> (mm)	ZOI in <i>E.coli</i> (mm)
+	Gentamycin(1 mg/ml)	44	30
-	Distilled water	-	-
<i>L.E.</i>	Leaf Extract	-	-
<i>B.E</i>	Bark Extract	-	-
6	AgNPs (B.E 25°C)	14	16
5	AgNPs (B.E 37°C)	20	14
2	AgNPs (B.E 80°C)	18	14
3	AgNPs (L.E 25°C)	22	20
1	AgNPs (L.E 37°C)	18	15
4	AgNPs (L.E 80°C)	-	-
AgNO ₃	AgNO ₃	18	14

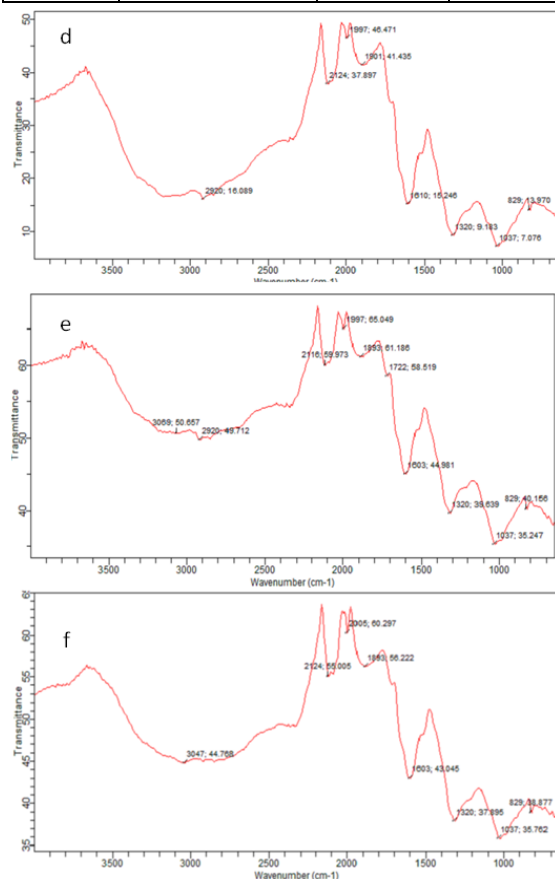


Figure 6. FTIR of AgNPs synthesized from Bark Extract (d)25°C, (e)37°C, (f) 80°C

AgNPs interact with bacterial cell walls individually or via the released Ag⁺ ions that generate “pits” on the cell walls owing to their nano size. This leads to the accumulation of AgNPs that begin to adhere strongly to the layers thereby releasing more Ag⁺. This phenomena strongly influences the destruction of Gram-positive bacteria due to the thicker PGN layer but the Gram negative bacteria are resistant to this phenomenon [24]. Hence, the present findings were in unison with the already published reports that AgNPs were more effective against *S. aureus* as compared to *E. coli*. According to Reidy et al. 2013, there are a series of mechanisms by which the AgNPs manifest the antibacterial property [25]. As nanoparticles have small size and large surface area they make strong contact with bacterial surface. It has been reported earlier that Ag-P III reduced the division in both *S. aureus* and *E. coli*. Secondly, the AgNPs penetrate the bacterial cell which leads to DNA damage. Thirdly, dissolution of AgNPs releases Ag⁺ ions that can act together with sulphur-containing proteins of bacteria to alter the structure and function.

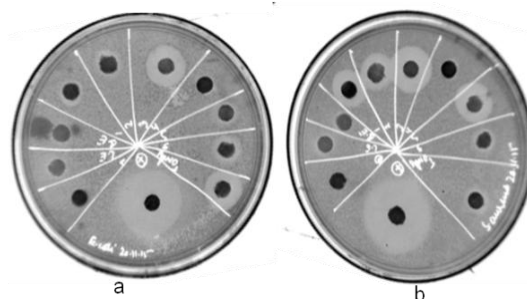


Figure 7. Disc diffusion Assay of AgNPs in a) *E. coli* b) *S. aureus*

This phenomenon is an important mechanism of the antimicrobial activity of AgNP. The interaction of dissolved Ag⁺ ions to an extracellular as well as

Table 3. Zone of inhibition (diameter in mm) of AgNPs at different concentrations synthesized from *S.cumini* leaves at 25°C

Sample	ZOI in <i>S.aureus</i> (mm)	ZOI in <i>E.coli</i> (mm)
+ve Gentamycin(1mg/ml)	30	34
-ve Distilled water	-	-
20mg/ml	22	26
10mg/ml	20	24
1mg/ml	17	20
100 µg/ml	16	16
10 µg/ml	14	-
1 µg/ml	13	-
100ng/ml	13	-

intracellular proteins highlights the binding of Ag⁺ ions with the thiol group present in vital enzymes that result in their inactivation or altered activity. Fourthly, Ag⁺ ions may further interact with the phosphorous containing compounds like DNA which undoubtedly interferes with its replication process and inhibits the proliferation resulting in decrease in growth over a period of time.

There have been reports in literature suggesting that the AgNPs synthesized from peel extract of *Dimocarpus Longan Lour* not only showed antibacterial activity against *S. aureus* and *E. coli*, but also showed cytotoxicity against PC-3 prostate cancer cells through a reduction in stat-3, bcl-2, survivin, as well as an increase in caspase-3 [26]. Anticancer activity of AgNPs has also been reported against human breast adenocarcinoma cell-line (MCF 7, MDA MB 231), cervical cancer (HeLa) as well as against oral epidermoid carcinoma (KB) cells at a concentration range of 6.25–50µg/ml. They were equally efficient against *Bacillus subtilis*, *Staphylococcus aureus*, *Salmonella typhimurium*,

Listeria monocytogenes and *Pseudomonas aeruginosa* with an IC₅₀ of 5–10µg/ml [4].

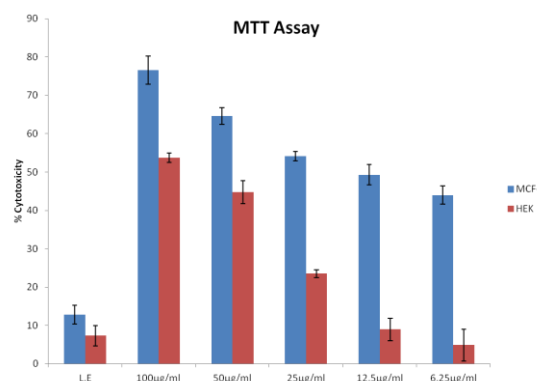


Figure 8. Graph showing percent Cytotoxicity of AgNPs against MCF-7 and HEK.

We report cytotoxicity of the Leaf extract (L.E.) and AgNPs at a single time point i.e. post 24 hrs of incubation with different concentrations. The percent cytotoxicity of L.E. and AgNPs against MCF-7 at concentration of 100 µg/ml, 50 µg/ml, 25 µg/ml, 12.5 µg/ml, 6.25 µg/ml was reported to be 12.77±2.43%, 76.6 ± 1.20%, 64.6 ± 2.32%, 54.1 ± 0.98%, 49.3 ± 2.87%, 44 ± 4.13%, respectively which is higher as compared to Human Embryonic kidney (HEK) cell line which is 7.32±2.68%, 53.67 ± 1.20%, 44.7 ± 2.96%, 23.5 ± 0.98%, 8.95 ± 2.87%, 4.89 ± 4.13%, respectively (Figure 8). The IC₅₀ value of bio-synthesized AgNPs from leaf extract of *S. cumini* against MCF-7 and HEK cells was found to be 12.50 µg/ml and 75.57 µg/ml, respectively in 24hrs. Similar reports have been published by Vivek et al. 2012, where in AgNP synthesized from *Annonas quamosa* showed cytotoxicity against MCF-7 cells at a concentration of 50µg/ml. The present results were in unison with the earlier published reports by Okafer et al proved that AgNPs is non-toxic at a concentration of 2–4 ppm to HEK cells [27]. Current findings provide a conclusive evidence of cytotoxic effects of biosynthesized AgNPs against MCF-7 cell-line as compared to HEK normal cell-line which indicated the specificity of AgNP against MCF-7.

In this study the expression of apoptotic protein was confirmed by western blotting, with β -actin as a standard for western blot analysis. Literature survey had proved that p53 (Figure 9) played a significant role in the cellular DNA damage responses and apoptosis induced by ROS [28].

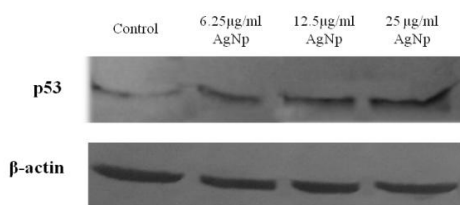


Figure 9. Western Blot showing the expression of p53 in MCF-7 at various concentrations of AgNPs in comparison to β -actin as a control.

Chemotherapeutics are usually aimed to target cancer cells *via* apoptosis, a multifaceted process harboring many effector molecules. p53 is a tumor suppressor gene acting by increasing the expression of pro-apoptotic genes simultaneously reducing the expression of anti-apoptotic genes like Bcl-2 [29]. The expression of p53 in MCF-7 cells (Figure 9). The present results were in unison with the reports published by Zhu et al where p53 levels were enhanced by AgNP treatment against HepG2 cells and also with Jang et al where

p53 levels were upregulated against MCF-7 [30-31].

4. CONCLUSION

We report cost effective, eco-friendly, safe, simple, non-toxic, and single step synthesis protocol for AgNPs from leaf and bark extracts of *Syzygium cumini*. The AgNPs made by leaf extract and that to at 25°C was found to be more active both in terms of antimicrobial and anticancer activity. The efficacy of AgNPs was evident in Gram positive bacteria at nanogram concentrations as compared to Gram negative bacteria, which suggested that these can prove to be very effective antimicrobial agents. MCF-7 cell line was susceptible to AgNPs and the cytotoxicity was probably *via* the upregulation of p53. These preliminary results warrant further experiments to elucidate the molecular mechanism both *in-vitro* and in *in-vivo* models. The proposed cost-effective, and eco-friendly approach for mass production of AgNPs has immense potential applications.

ACKNOWLEDGEMENT

Disha Mittal is thankful to University Grants Commission (UGC) for her JRF and Ankita Leekha is thankful to Department of Biotechnology (DBT) for her SRF

REFERENCES

1. Yu R., Wu J., Liu M., Zhu G., Chen L., Chang Y., Lu H., (2016). "Toxicity of binary mixtures of metal oxide nanoparticles to *Nitrosomonas europaea*", *Chemosphere*, 153: 187-197.
2. Vadlapudi V., Kaladhar D.S.V.G.K., (2014). "Review: Green Synthesis of Silver and Gold Nanoparticles", *M.E.J.S.R.*, 19: 834-842.
3. Ahmed B. A., Raman T., Anbazhagan V., (2016). "Platinum nanoparticles inhibit bacteria proliferation and rescue zebrafish from bacterial infection", *RSC Adv*, 6: 44415-44424.
4. Barua S., Banerjee P. P., Sadhu A., Sengupta A., Chatterjee S., Sarkar S., Karak N., (2017). "Silver Nanoparticles as Antibacterial and Anticancer Materials against Human Breast, Cervical and Oral Cancer Cells", *J.N.N.*, 17: 968-976.
5. Liu Y. C., Lin L.H., (2004). "New pathway for the synthesis of ultrafine silver nanoparticle from bulk silver substrates in aqueous solutions by sono-electrochemical methods", *Electrochem. Commun.*, 6: 1163-1168.
6. Tan Y., Wang Y., Jiang L., Zhu D., (2002). "Thiosalicylic acid-functionalized silver nanoparticles synthesized in one-phase system", *J. Colloid and Interface Sci.*, 249: 336-345.
7. Smetana A. B., Klabunde K. J., Sorensen C. M., (2005). "Synthesis of spherical silver nanoparticles by digestive ripening, stabilization with various agents, and their 3-D and 2-D superlattice formation", *J. Colloid and Interface Sci.*, 284: 521-526.

8. Mallick K., Witcomb M., Scurrill M. S., (2005). "Green Nanotechnology for Biofuel Production", *Mater. Chem. Phys.*, 90: 221.
9. Srikar S.K., Giri D.D., Pal D.B., Mishra P.K., Upadhyay S.N., (2016). "Green Synthesis of Silver Nanoparticles: A Review", *Green Sustain Chem.*, 6(01): 34.
10. Remya V.R., Abitha V.K., Rajput P.S., Rane A.V., Dutta A., (2017). "Silver nanoparticles green synthesis: A mini review", *Chemistry International.*, 3(2): 165-171.
11. Iravani S., (2011). "Green synthesis of metal nanoparticles using plants", *Green Chem.*, 13(10): 2638-2650.
12. Swami S.B., Thakor N.S.J., Patil M.M., Haldankar P.M., (2012). "Jamun (*Syzygium cumini* (L.): A Review of Its Food and Medicinal Uses", *Food Nutr. Sci.*, 3(08): 1100.
13. Dey A., Dasgupta A., Kumar V., Tyagi A., Verma A.K., (2015). "Evaluation of antibacterial efficacy of polyvinylpyrrolidone (PVP) and tri-sodium citrate (TSC) silver Nanoparticles", *Int. Nano. Lett.*, 5(4): 223-230.
14. Tyagi A., Agarwal S., Leekha A., Verma A.K., (2014). "Biodistribution and *in-vivo* Efficacy of Doxorubicin Loaded Chitosan Nanoparticles in Ehrlich Ascites Carcinoma (EAC) bearing Balb/c mice", *Int. J. Adv. Res.*, 2: 357.
15. Blancher, C., Jones, A. (2001) "SDS -PAGE and Western Blotting Technique in S. A. Brooks & U. Schumacher, ed. by Metastasis Research Protocols", Vol I: Analysis of Cells and Tissues Totowa, NJ: Humana Press; p.145.
16. Vivek R., Thangam R., Muthuchelian K., Gunasekaran P., Kaveri K., Kannan S., (2012). "Green biosynthesis of silver nanoparticles from *Annona squamosa* leaf extract and its *in vitro* cytotoxic effect on MCF-7 cells", *Process Biochem.*, 47(12): 2405-2410.
17. Gurunathan S., Raman J., Malek S. N., John P. A., Vikineswary S., (2013). "Green synthesis of silver nanoparticles using *Ganoderma neo-japanicum* Imazeki: a potential cytotoxic agent against breast cancer", *Int. J. Nanomedicine.*, 8: 4399.
18. Singh A., Jain D., Daima H.K., Kachhwaha S., Kothari S. L., (2010). "Green synthesis of silver nanoparticles using argemone mexicana leaf extract and evaluation of their antimicrobial activities" *Dig J. Nanomater. Biostruct.*, 5(2): 483-489.
19. Begum N. A., Mondal S., Basu S., Lasker R. A., Mandal D., (2009). "Biogenic synthesis of Au and Ag nanoparticles using aqueous solutions of Black Tea leaf extracts", *J. Colloids and Surf. B Biointerfaces*, 71(1): 113-118.
20. Sathyavathi R., Krishna M. B., Rao S. V., Saritha R., Rao D. N., (2010). "Biosynthesis of Silver Nanoparticles Using *Coriandrum Sativum* Leaf Extract and Their Application in Nonlinear Optics"; *Adv. Sci. Lett.*, 3: 138-143.
21. Cumberland S. A., Lead J. R., (2009). "Particle size distributions of silver nanoparticles at environmentally relevant conditions", *J. Chromatogra.*, 1216(52): 9099-9105.
22. Siddig M. A., Abdelgadir E. A., Elbadawi A. A., Mustafal M. E., Mussa A. A., (2015). "Structural characterization and physical properties of *Syzygium cumini* flowering plant", *Int.J. Innov. Res. Sci. Eng.*, 4: 2694.
23. Prabhu S., Poulouse E. K., (2012). "Silver Nanoparticles: mechanism of antimicrobial action, synthesis, medical applications and toxicity effects", *Int. Nan. Lett.*, 2(1): 32.
24. Mirzajani F., Ghassempour A., (2011). "Antibacterial effect of silver nanoparticles on *Staphylococcus aureus*", *Res. Microbio.*, 162(5): 542-549.
25. Reidy B., Haase A., Luch A., Dawson K. A., Lynch I., (2013). "Mechanisms of Silver Nanoparticle Release, Transformation and Toxicity: A Critical Review of Current Knowledge and Recommendations for Future Studies and Applications", *Materials*, 6(6): 2295-2350.
26. He Y., Du Z., Ma S., Cheng S., Jiang S., Liu Y., Zheng X., (2016). "Biosynthesis, Antibacterial Activity and Anticancer Effects Against Prostate Cancer (PC-3) Cells of Silver Nanoparticles Using *Dimocarpus Longan* Lour. Peel Extract" *Nanoscale Res. Lett.*, 11(1): 300.
27. Okafor F., Janen A., Kukhtareya T., Edwards V., Curley M., (2013). "Green synthesis of silver nanoparticles, their characterisation, application and antibacterial activity", *Int. J. Environ. Res. Public Health.*; 10(10): 5221-5238.
28. Gurunathan S., Park J. H., Han J. W., Kim J. H., (2015). "Dual functions of silver nanoparticles in F9 teratocarcinoma stem cells, a suitable model for evaluating cytotoxicity and differentiation-mediated cancer therapy", *Int. J. Nanomedicine.*; 10: 4203.
29. Ricci M. S., Zong W. X., (2006). "Chemotherapeutic approaches for targeting cell death pathways", *Oncologist.*, 11(4):342-357.
30. Zhu B., Li Y., Lin Z., Zhao M., Xu T., Wang C., Deng N., (2016). "Silver Nanoparticles Induce HePG-2 Cells Apoptosis Through ROS-Mediated Signaling Pathways", *Nanoscale Res. Lett.*, 11(1): 198.
31. Jang S. J., Yang I. J., Tettey C. O., Kim K. M., Shin H. M., (2016). "Green Silver Nanoparticles: Novel Therapeutic Potential for Cancer and Microbial Infections", *Materials Science and Engineering*, 68: 430.